The Iraqi Journal For Mechanical And Material Engineering, Vol.17, No2,July 2017

THE MICROSTRUCTURE AND MAGNETIC CHARACTERIZATION OF NICKEL FERRITE NANOFIBERS

Dr. Fadhil A. Chayad
University of Technology
Dept. of Materials Eng.

Dr. Akram R. Jabur
University of Technology
Dept. of Materials Eng.

Shaima'a J. Kareem
Babylon University
Eng. Materials College.
shaimaa.kareem@gmail.com

ABSTRACT:

The nanofibers of nickel ferrite ($NiFe_2O_4$) was prepared by electrospinning technique. Nickel nitrate hexahydrate, iron nitrate nonahydrate, Polyvinylpyrrolidone (PVP) and N-dimethylformamide (DMF) were used as precursor materials. Crystallization behavior of the nanofibers was studied by X-ray diffraction (XRD). Nanofibers phases can change from amorphous to spinel ferrite depending on the calcination temperature at (500°C, 600°C, 700 °C) and crystallite size by Scherrer's formula about (18.26 – 28.10) nm, while morphological and structural properties were investigated by scanning electron microscopy (SEM). Magnetization measurements were carried out on a vibrating sample magenometer (VSM), which revealed saturation magnetization of the samples were strongly dependent on the calcination temperature. Finally, our results showed that the electrospinning method leads to obtain nanofibers of nickel ferrite with good controllable stoichiometry at low temperature.

KEY WORDS : nanofibers, ferrite, electrospinning, nickel, FE-SEM, XRD, VSM.

الخصائص التركيبية والمغناطيسية لألياف النيكل – الفيرايت النانوية

فاضل عطية جياد
الجامعة التكنولوجية
قسم هندسة المواد

أكرم رحيم جبر
الجامعة التكنولوجية
قسم هندسة المواد

شيماء جابر كريم
جامعة بابل
كلية هندسة المواد

الخلاصة

تم تحضير الياف النيكل – الفيرايت النانوية بواسطة تقنية البرم الكهربائي. تضمن تحضير المحلول المناسب لجهاز البرم الالكتروني من نترات النيكل المائية ($Ni (NO_3)_2.6H_2O$) و نترات الحديد ($Fe (NO_3)_2.9H_2O$) وبوليمر بولي فينل بيروليدون(PVP) تذاب بواسطة المذيب $DMF(C_3H_8O_2)$. السلوك البلوري للالياف الناوية الناتجة تم دراستها بواسطة تحليل الاشعة السينية، حيث وجد اطوار الالياف النانوية تتحول من التركيب العشوائي الى الفيرايت السبنلي البلوري معتمدة على درجة حرارة الحرق (700°C, 600°C, 500 °C) اما قطر البلورة فتم حسابها بواسطة معادلة شيرر Scherrer's formula وكان حوالي nm (18.26 – 28.10). الخواص الشكل والبناء الداخلي لألياف تم بيانها بواسطة المجهر الالكتروني الماسح FE–SEM، اما القياسات المغناطيسية نفذت بواسطة مقياس الاهتزاز المغناطيسي (VSM) والتي أظهرت ان الفيض المغناطيسي يعتمد بصورة رئيسية على درجة حرارة الحرق للالياف. واخيرا النتائج بينت ان تقنية البرم الكهربائي ملائمة لإنتاج الياف النيكل – الفيرايت النانوية بدرجات الحرارة المنخفضة .

الكلمات المفتاحية: الياف نانوية، الفيرايت، البرم الكهربائي، النيكل، تحليل الاشعة السينية، المجهر الالكتروني الماسح .

Received:14-4-2016
Accepted:8-5-2016

INTRODUCTION :-

Nanoscale have basic kinds of building blocks first zero-dimensional materials (0D) included nanoparticles, nano-clusters, and nanocrystals. Second unidimensional ones (1D) contained nanowires, nanofibers, and nanotubes [Moreno, Ferrari, 2011] .

Nanoparticles are quasi-zero-dimensional (0D) in which all characteristic linear dimensions are of the same order of magnitude that means the shape of nanoparticles like spheroids, as a rule [Gubin,2009][Gubin, et al, 2005] . **Nanofibers** are fibers have a diameter less than 1 micron. In a few years, nanofiber has become very important for scientists and companies because of its characteristics like very small diameter, tiny pore size, large surface area, etc. [Cengiz, et al., 2009].

Ferrites find potential applications for making many devices such as permanent magnets, memory storage devices, microwave devices, and for the telecommunication equipment purpose. The importance of ferrites lies in the fact that they possess wide range of electrical and magnetic properties [Goldman, 2006].

The general formula of ferrite is $M'M''_2O_4$, where M' is a divalent metal ions such as (Fe^{2+}, Mg^{2+}, Ni^{2+}, Co^{2+}, Zn^{2+}, Cu^{2+}) and M'' is iron, chromium, manganese, etc. (trivalent metal ions); that is, Fe^{3+}, Cr^{3+}, Al^{3+}, Mn^{3+} [Srivastava, et al., 2012].

The ferrites are involved dominant compound of Fe_2O_3, are contained three groups namely Spinal, Garnet, and hexagonal ferrites [Goldman, 2006] . **Normal** spinel structure, where all Me^{2+} ions occupy A sites; structural formula of such ferrites is Me^{2+} $[Fe_2^{3+}]$ O_4^{2-}. This type of distribution takes place in zinc ferrites Zn^{2+} $[Fe^{2+}Fe^{3+}]$ O_4^{2-} [Mastai, 2012].Inversed spinel structure, where all Me^{2+} are in B-positions and Fe^{3+} ions are equally distributed between A and B-sites: structural formula of these ferrites are $Fe^{3+}[Me^{2+}Fe^{3+}]$ O_4^{2-}. Magnetite Fe_3O_4, ferrites $NiFe_2O_4$ and $CoFe_2O_4$ have inversed spinel structure. Mixed spinel structure, when cations Me^{2+} and Fe^{3+} occupy both A and B positions; structural formula of this ferrite is $Me_{1-x}{}^{2+}Fe_x{}^{3+}$ $[Me_x{}^{2+}Fe_{2-x}{}^{3+}]$ O_4^{2-}, where x is the degree of inversion [George, Juang, 2006] . **The** spinel structure in which the sites occupied by the cations are of two types, tetrahedral and octahedral sites. The compositional variation in these ferrites results in the redistribution of metal ions over the tetrahedral and octahedral sites, which can modify the properties of ferrites. The physical properties of these ferrite nanoparticles can be also designed by changing the parameters such as composition or by the synthesis method. There are various methods for the synthesis of ferrite nanoparticles, which includes sol-gel, oxidation, hydrothermal, ball milling and chemical co-precipitation method [Morrison, et al., 2004]. B. P. Jacob, et al, have prepared very small size of nanoparticles of Nickel ferrite of by using sol–gel combustion and co-precipitation techniques [Jacob, et al, 2011]. M. G. Naseri, et al, have synthesized nanocrystals of Nickel ferrite from metal nitrates with various of concentrations of PVP for comparison and in the absence of PVP as an aqueous solution, followed by calcination process at different temperatures from (623 to 823)] [Naseri, et al., 2013]. A. Kumar, et al, have synthesizes a series of nickel doped zinc ferrite $Ni_xZn_{1-x}Fe_2O_4$ $(0 \leq x \leq 0.6)$ nanoparticles by using sol-gel process [Kumar, et al., 2015,] . **Electrospinning** is one of the simplest methods to produce very fine fibers from a precursor solution or liquid. Electrospinning has explored as a high efficiency method for the generation of 1D ceramic nanofibers. Materials in nanofiber form have an exceptionally high specific surface area, which enables a high proportion of atoms to be on the fiber surface. This will result in quantum efficiency, nanoscale effect of unusually high surface energy, surface reactivity, high thermal and electrical conductivity, and high strength [He, et al., 2008].

In this search, the nano nickel-zinc ferrite ($NiFe_2O_4$) has fabricated using the electrospinning process of sol–gel solution. There are few studies of nickel ferrite by electrospinning technique. S. Maensiri, et al, have fabricated and calcinated the as-spun $MgFe_2O_4$/ PVP composite nanofibers at (500–800) ºC in air for 2 h resulted in developed spinel ($MgFe_2O_4$) magnesium nanoferrite. Nanoparticles ($MgFe_2O_4$) crystallite size increased from 15 ± 4 to 24 ± 3 nm with increasing calcination temperature from (500 to 800)ºC. Results of magnetization showed a ferromagnetic behavior of the calcinated composite nanofibers, which showed an increasing in the tendency of (Ms) with the enhancement of crystallinity, and crystallite size [Maensiri, et al, 2009].

S. Nilmoung, et al, have successfully fabricated Carbon/$NiFe_2O_4$ composite nanofibers with polyacrylonitrile (PAN) by using electrospinning method. The morphologies and the crystal size of as-spun and carbonized composite samples have influenced the stabilization time and the carbonization temperature (800-900-1000) ºC. Carbonization in argon atmosphere at 1000 ºC to PAN/$NiFe_2O_4$ formed full phase of $NiFe_2O_4$ embedded carbon fibers. The samples stabilized at 280 ºC for 0.5 h and 2 h had the average crystallite size was (30.9 and 30.1) nm and showed ferromagnetism behavior having saturation magnetizations (Ms) of (0.36 and 3.40) emu/g, respectively [Nilmoung, et al, 2009]. X. Jun, et al, have prepared Ni- Zn ferrite/ polyvinylpyrrolidone composite fibers by sol–gel assisted electrospinning. $Ni_{0.5}Zn_{0.5}Fe_2O_4$ nanofibers had pure cubic spinel structure effected subsequently by calcination temperatures. The magnetic behavior found that the grain sizes of the nanofibers increase significantly and the nanofibers morphology gradually transforms from a porous structure to a necklace-like nanostructure with the increase of calcination temperature. The $Ni_{0.5}Zn_{0.5}Fe_2O_4$ nanofibers obtained at 1000 ◦C for 2 h are characterized by a necklace-like morphology and diameters of 100–200 nm. Ms of the random nanofibers is increased when the calcination temperature increased. Hc reached a maximum at a calcination temperature of 600 ◦C. Due to the shape anisotropy, the aligned nanofibers exhibited an obvious magnetic anisotropy and the ease magnetizing direction was parallel to the nanofibers axis. [Jun, et al., 2009]

MATERIALS AND METHODS :-

Materials

The raw materials used in this study are presented in **Table (1)**.

Synthesis of $NiFe_2$ O_4 ferrite nanofibers

In this study, the Fe_2O_4 ferrite nanofibers was synthesized by sol-gel based electrospinning. The starting materials $Ni(NO_3)_2.6H_2O$ mixed with Fe $(NO_3)_2.9H_2O$ and dissolved in DMF ($C_3H_8O_2$) for 2hrs by using hot plate magnetic stirrer, type (Stuart SB 162-3, England), with an initial ratio of Ni to Fe of [1: 2]. After a period of aging, 4g polyvinylpyrrolidone (PVP) was added to the solution, which is then stirred continuously for 4hrs, resulting in a homogeneous $NiFe_2O_4$ precursor solution.

Electrospinning process :

By using electrospinning device, type (NaBond, Nano-fiber, Electro-spinning Unit installation guide, China), the precursor solution of composite $NiFe_2O_4$ /PVP are loaded into a syringe (10 ml) with a stainless steel needle and the distance between needle stage and dram type collector was (15cm). High voltage (20 KV) was supplied to the needle to create a potential difference between the needle and the collector, while the flow rate of solution was (0.3 ml/hr) at room temperature.

Drying and Firing processes

The thin film of ferrite/ PVP composite nanofibers formed by electrospinning process, which allowed to the initial ferrite particles, which are deposited on the surface and inside the nanofibers of thin film. To obtain the powder of $NiFe_2O_4$ ferrite must be remove PVP from the as-spun nanofibers, so the thin film dried at 250 ºC for 2h by using porcelain basin using oven dryer type (memmert Gmbh+Co.KG, universal oven (UIS),Germany). The dried $NiFe_2O_4$ ferrite heated at (500°C, 600°C, 700 ºC) for 2h in air by using furnace to obtain the NFO nanofiber by using Furnace up to 1600°C for pyrolysis, type (Protherm, Turky). The heating rate was kept at 5 ºC/min.

Characterizations:

The structure of the $NiFe_2O_4$ nanoparticles was characterized by the X-ray diffraction (XRD), type (Shimadzo, XRD6000, diffractometer, Japan). X-rays are generated using Copper (Cu-Kα) radiation at 30 kV, 40 mA and wavelength ($\lambda = 1.5406$ Å), radiation to generate diffraction patterns from powder crystalline samples at ambient temperature in a 2θ range of 10° to 70°. The microstructure and particle size of the nanocrystals were investigated by scanning electron microscopy (FE-SEM) with energy dispersive X-ray spectroscopy (EDS), type (MIRA3 TESCAN- RMRC) (TM - 1000 Hitachi tabletop Japan). Magnetization measurements were conducted using a vibrating sample magnetometer (VSM), model (Mdkft), type (Danesh-pajoohe kashan Co. - Iran), at room temperature

RUSTLES AND DISCUSSION :

XRD Aanalysis :

Generally, XRD can be used to characterize the crystallinity of nanoparticles. **Fig. (1)** is shown XRD patterns of nickel zinc ferrite powder samples after being calcined at (500°C, 600°C, 700 ºC) for 2 hour, comparing with standard JCDPS card. The d values and intensities of observed diffraction peaks matches well with JCPDS card no. 52-0278 of the nickel ferrite having Fd-3m space group. It gives the major phases in all preparations was the spinel phase (Nickel ferrite) at the peaks (220), (311), (222), (400), (422), (511), and (440). It is the only phase ($NiFeO_4$) appeared in all the prepared samples. No foreign phases are detected, proving the phase purity of the samples.

At increasing the calcination temperatures, causes the peaks will become sharper and narrow, and this reflects a higher crystallinity and increase the grain size. The conventional methods are needed to high calcination temperatures and long heating time [Nilmoung, et al., 2009], by electrospinning method, ferrite phase can be produced at low temperature and short time [Jun, et al., 2009]. The crystallite size were characterized by XRD for structural determination and estimation of crystallite size by using Scherrer's formula at the peak (311) :

$$D_{XRD} = 0.89\, \lambda / \beta \cos\theta \qquad (1)$$

Where λ is wavelength of X-ray radiation used in Å, θ is the diffraction angle, β is the full width at half maximum (FWHM) in radians in the 2θ scale, D_{XRD} is the crystallite size in nm

[Cullity, 1967]. These measurements show the increasing in crystallite size of nickel ferrite with increasing calcination temperatures around (18.26 – 28.10) nm.

The lattice parameter of the as-prepared sample, according to the cubic crystal structure was calculated from the main peak of spinel structure (311) using equation:

$$a = d\sqrt{h^2 + k^2 + l^2} \qquad (2)$$

where “d” is the interplanar distance, “h, k and l” are the miller indices and “a” is the lattice parameter [Fultz, Howe, 2013]. The changing in parameter (a) is obviously explained the fluctuation in the size of nickel ferrite structure because of increasing the calcination temperatures. The structural parameters calculated from the diffraction pattern shown in **Table 2**.

FE- Scanning Electron Microscopy (Fe-SEM) analysis:

The scanning electron microscope (FE- SEM) used to study the surface morphology of resulted nanofibers. **Fig. (2)** is explained the FE-SEM images for $NiFeO_4$ samples calcined at (500- 600 -700) °C, from this technique can calculate the grain size, which formed nanofibers of samples, which shown in rang of (24.51-44.76) nm.

The surface of dried $NiFe_2O_4$/PVP composite fibers is smooth due to the amorphous nature of the composite fibers and their diameters. The fiber diameters gradually decrease with increasing calcination temperature. The fiber surface shrinks and becomes largely porous owing to the evaporation of PVP and crystallization of spinel, and the pores on fiber surfaces disappear and the fiber diameters decreased. The cross section of the fibers obtained at this temperature is composed of only several grains. The fiber morphology gradually transforms from a porous structure to a necklace-like nanostructure due to growth of the ferrite grains. When calcination temperature increases, the fibers are mainly necklace-like well-crystallized nanofibers. The formation of necklace-like morphology may be attributed to the asymmetric shrinkage of spinel during the thermal decomposition and crystallization process of composite fibers. At the time, rapid of growth grains occurs during calcinations at high temperatures, then the nanofibers will be unstable and droop grain boundary occurs to relieve the strain energy [Lu, et al., 2006].

The formation of necklace-like nanofibers in samples, which clearly appeared in FE-SEM images for nickel ferrite ($NiFe_2O_4$) samples calcinated at (500 °C, 600 °C, 700 ºC) for 2 hours.

From FE-SEM, images can notice the grains size increased with calcination temperature increased and after the necklace-like crystallized nanofibers formed. Also can calculated the diameters of nanofibers around (~ 80 to 200 nm) and the length of fibers around (~ 1 to higher of 10 μm).

Fig. (3) is revealed the chemical identify of ($NiFe_2O_4$) nanofibers, which is formed by electrospinning technique and calcinated at (500 °C, 700 ºC) for 2 hours. This analysis is achieved by EDX technique .

Vibrating Samples Magnometer (VSM) measurement:

Magnetic characterization of the samples are performed by VSM at room temperature with a maximum applied field of 10 kOe. **Fig. (4)** is shown typical magnetic hysteresis loops of nickel ferrite ($NiFe_2O_4$) samples prepared by electrospinning method and calcinated at (500 – 600 -700) °C. The saturation of magnetic values are affected by increasing the calcination temperature because of gradual increase in crystallinity and particle size [Moeen, et al., 2010]. The saturation magnetization (Ms) is increased as calcination temperature increases. This phenomenon may be attributed to the enhancement of the fiber purity and crystallinity and a decreasing proportion of the pinned surface magnetic moments in overall magnetization as the nanocrystals grow in size[Jun, et al., 2009][Song, Zhang, 2004], that as shown **Table (3)**.

When the calcination temperature is increased, the nanocrystals contained in fibers are larger than the single-domain size and reach multi-domains due to the increase in grain size, and the formation of domain walls will cause the coercivity to decrease [Jun, et al., 2009][Maaz, et al., 2007].

The decreasing of coercivity is usually attributed to a switch of the magnetization process from domain rotation to domain wall motion. At the same time, with further increase in the calcination temperature, the concentration of impurities and defects of these nanofibers will gradually decrease, because there is an improvement in the nanofibers crystallization, and will be reduce the resistance of domain wall motion and consequently leads to a monotonous decrease in coercivity [Jun, et al., 2009] [Jun, et al., 2009].

The magnetization is depended on particle size that the smaller particles have the higher the remnant magnetization. This is led to the smaller particles act as a single magnetic domains, whereas larger particles work as multiple domains [Nilmoung, et al., 2009].

CONCLUSIONS :-

The nanofibers of nickel-zinc ferrite ($NiFe_2O_4$) calcined at (500, 600, and 700) ◦C for 2 h, was prepared by electrospinning technique with a pure cubic spinel structure. The morphology and diameters of the fibers are largely affected by the calcination temperature. With increasing calcination temperature, the morphology of the calcined fibers gradually transforms from a porous structure to a necklace-like nanostructure. The $NiFe_2O_4$ fibers are mainly necklace like nanofibers with diameters around (~ 80 to 200 nm) and the length of fibers around (~ 1 more than 10 μm). The magnetic measurements are shown that the saturation magnetization of the nickel ferrite nanofibers increases with increasing temperature, while the coercivity decrease as the calcination temperature increase. The aligned $NiFe_2O_4$ nanofibers are exhibited soft ferrite with cubic spinel structure.

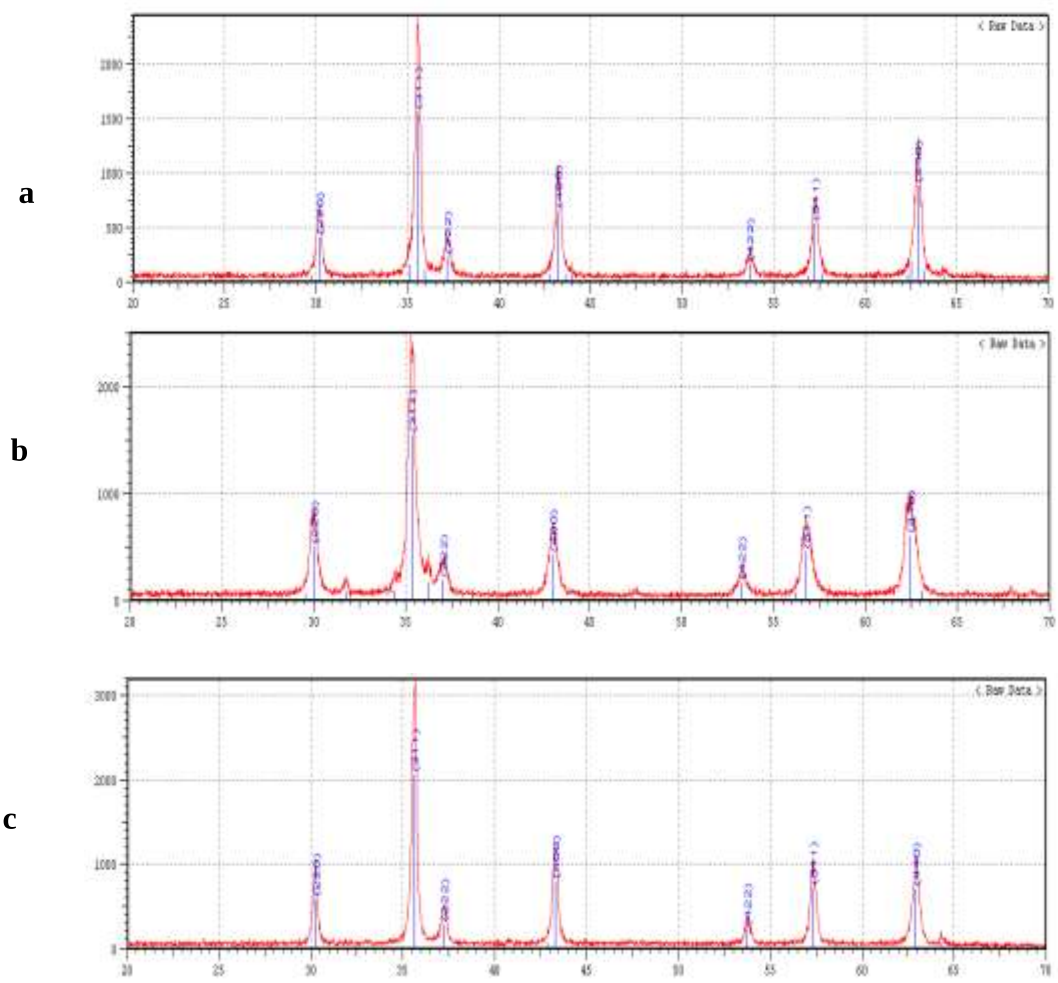

Figure (1): XRD patterns of nickel ferrite ($NiFe_2O_4$) samples calcinated at:
a- 500 °C, b- 600 °C, c- 700 °C

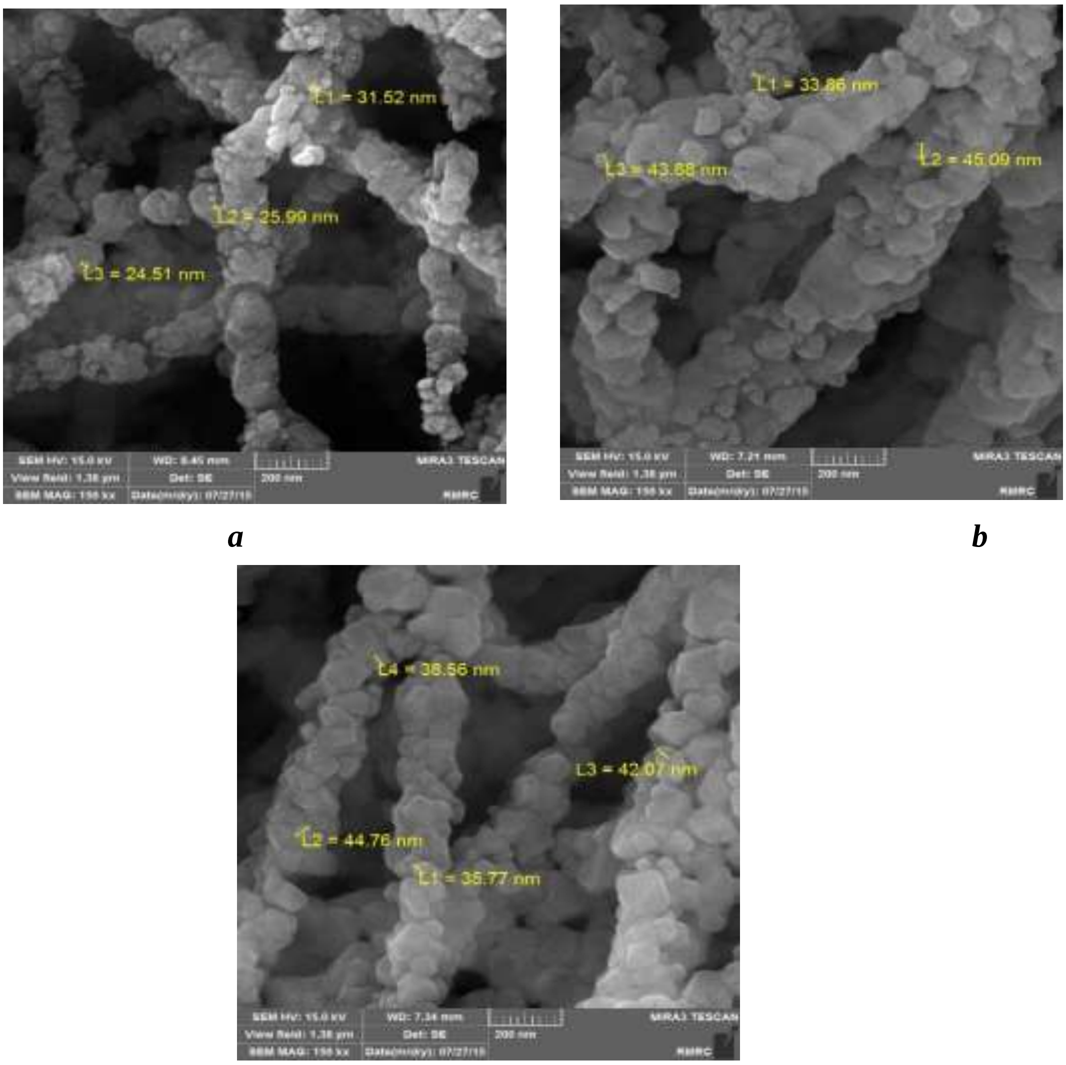

a *b*

c

Figure (2): FE-SEM images of nickel ferrite ($NiFe_2O_4$) sample calcinated at:
a- 500 °C, b- 600 °C, c- 700 °C

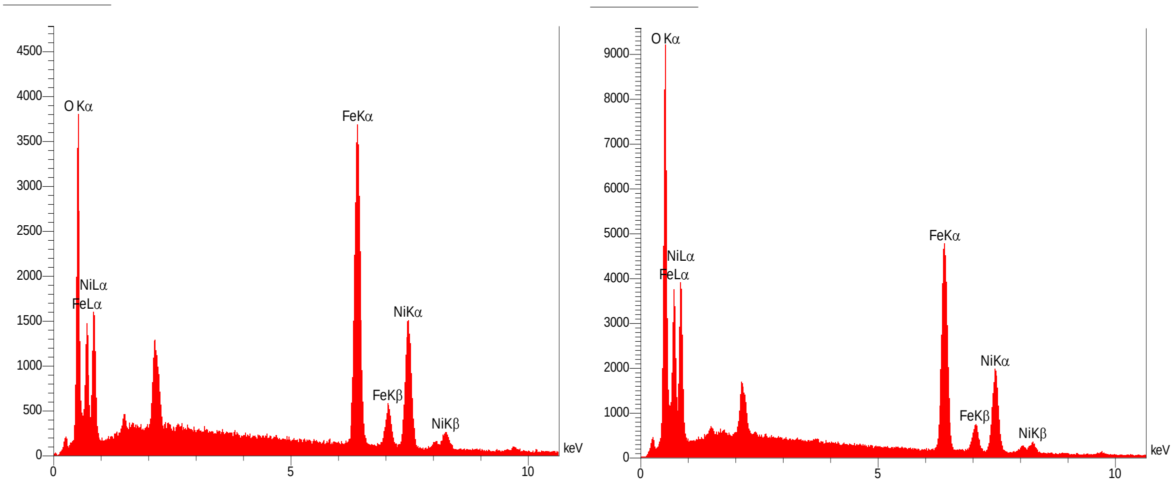

a **b**

Figure (3): EDX of nickel ferrite ($NiFe_2O_4$) samples calcinated at:
a- 500 °C , b- 700 °C

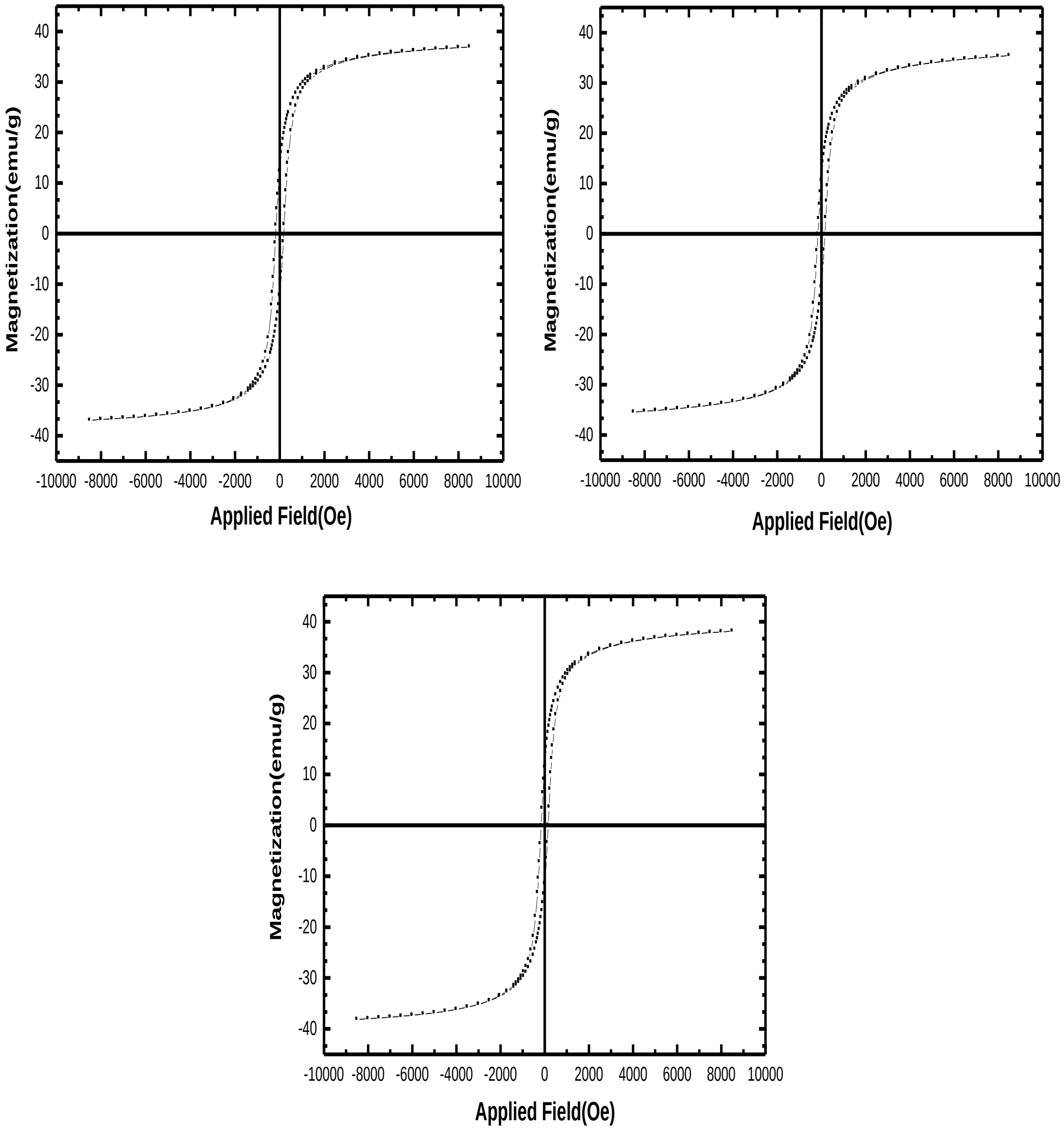

(c)

Figure (4): Room temperature hysteresis loop of nickel ferrite ($NiFe_2O_4$) samples calcinated at:
a- 500 °C, b- 600 °C, c- 700 °C

Table (1) the raw materials used.

Raw materials	Formulation	Molecular weight (g/mol)	Purity %	Physical state	Origin manufacturing
Iron (III) nitrate nonahydrate	$Fe (NO_3)_3.9H_2O$	404.00	99	Solid	China
Nickel nitrate hexahydrate	$Ni(NO_3)_2.6H_2O$	290.79	99.5	Solid	China
Polyvinylpyrrolidone	$(C_6H_9NO)_n$	30 k	99.9	Solid	China
N,N-dimethylformamide DMF	$C_3H_8O_2$	73.8	99.9	Liquid	India

Table (2) the structural parameters of $NiFe_2O_4$ calcinated at (500 -600 – 700) °C.

Calcination temp.(°C)	D_{XRD} (nm)	a (Å)
500	18.26	8.41
600	26.24	8.36
700	28.10	8.34

Table (3) Magnetic properties of $NiFe_2O_4$ nanofibers

Calcination temp.(°C)	Ms (emu/g)	Mr (emu/g)	Hc(Oe)
500	34.203	14.867	179.181
600	35.479	13.008	166.382
700	37.081	13.752	162.116

REFERECNCES :

Cengiz F., I. Krucińska, E. Gliścińska, M. Chrzanowski, and F. Göktepe, 2009, Comparative Analysis of Various Electrospinning Methods of Nanofibre Formation, FIBRES & TEXTILES in Eastern Europe, Vol. 17, No. 1 (72) pp. 13-19 .

Cullity B. D., 1967, Elements of X-ray Diffraction, Adison-Wesley Publ. Co., London .

Fultz B., and J. Howe, 2013, Transmission Electron Microscopy and Diffractometry of Materials, Graduate Texts in Physics, Springer-Verlag Berlin Heidelberg .

George D.A., and R.SH. Juang, 2006, An Overview of the Structure and Magnetism of Spinel Ferrite Nanoparticles and Their Synthesis in Microemulsions, the Chemical Engineering Journal, pp. 51-65.

Goldman A., 2006, Modren Ferrite Technology, 2nd edition, Springer Science& Business Media, Inc.,

Gubin S P, Yu A Koksharov, G B Khomutov, and G Yu Yurkov, 2005, Magnetic nanoparticles: preparation, structure and properties, Russian Academy of Sciences and Turpion Ltd .

Gubin S.P, 2009, Magnetic Nanoparticles, WILEY-VCH Verlag GmbH & Co.KGaA, Weinheim, pp. 1-2 .

He J. H., Y. Liu, L. F. Mo,Y. Q. Wan, and L. Xu, 2008, Electrospun Nanofibers and Their Applications, iSmithers, Shawbury, Shrewsbury, Shropshire, SY4 4NR, UK .

Jacob B. P, A. Kumar, R. P Pant, S. Singh, and E. M Mohammed, 2011, Influence of preparation method on structural and magneticbproperties of nickel ferrite nanoparticles, Indian Academy of Sciences, Bull. Mater. Sci., Vol. 34, No. 7, pp. 1345-1350 .

Jun Xi., S. Xiang-Qian, S. Fu-Zhan, and L. Ming-Quan, 2009, Fabrication and magnetic properties of $Ni_{0.5}Zn_{0.5}Fe_2O_4$ nanofibers by electrospinning, Chin. Phys.Soc. and IOP Publishing Ltd, Vol18 No 11.

Kumar A., P. Kumar, G. Rana, M. S. Yadav and R. P. Pant, 2015, A study on structural and magnetic properties of $Ni_xZn_{1-x}Fe_2O_4$ ($0 \leq x \leq 0.6$) ferrite nanoparticles, Appl. Sci. Lett. 1(2), pp. 33-36 .

Lu X., D. Zhang, Q. Zhao, C. Wang, W. Zhang, and Y. Wei, 2006, Large-Scale Synthesis of Necklace-Like Single-Crystalline $PbTiO_3$ Nanowires, WILEY-VCH Verlag GmbH & Co. KGaA, Weinheim, Macromol, Rapid Commun, pp. 76–80 .

Maaz K, Arif Mumtaz,, S.K. Hasanaina, and Abdullah Ceylan, 2007, Synthesis and magnetic properties of cobalt ferrite ($CoFe_2O_4$) nanoparticles prepared by wet chemical route, Elsevier, Journal of Magnetism and Magnetic Materials, pp. 289–295 .

Maensiri S., M. Sangmanee, and A. Wiengmoon, 2009, Magnesium Ferrite ($MgFe_2O_4$) Nanostructures Fabricated by Electrospinning, Nanoscale Res Lett, pp. 4:221–228 .

Mastai Y., 2012, Crystalization in Spinel Ferrite Nanoparticles, Advances in Crystallization Processes, ISBN: 978-953-51-0581-7, InTech, pp. 350-380 .

Moeen Sh. J, M. R. Vaezi, and A. A. Yousefi, 2010, Chemical Synthesis of Nano-Crystalline Nickel-Zinc Ferrite as a Magnetic Pigment, Prog. Color Colorants Coat, pp. (3) 9-17 .

Moreno R., and B. Ferrari, 2011, Nanoparticles Dispersion and the Effect of Related Parameters in the EPD Kinetics, Springer, pp.73-81.

Morrison S. A., C. L. Cahill, E. E. Carpenter, S. Calvin, R. Swaminathan, M. E. McHenry, and Vincent G. Harris, 2004, Magnetic and structural properties of nickel zinc ferrite nanoparticles synthesized at room temperature, J. Appl. Phys., Vol. 95, No. 11, pp. 6393-6395 .

Naseri M. G., E. Saion, and N. K. Zadeh, 2013, The amazing effects and role of PVP on the crystallinity, phase composition and morphology of nickel ferrite nanoparticles prepared by thermal treatment method, International Nano Letters, 3:19.

Nilmoung S., S. Rugmai, and S. Maensiri, 2009, Fabrication, Structure, and Magnetic Properties of Carbon/Nickel Ferrite ($NiFe_2O_4$) Composite Nanofibers", 18th International Conference on Composite Materials .

Song Q., and Z. J Zhang, 2004, Shape Control and Associated Magnetic Properties of Spinel Cobalt Ferrite Nanocrystals, J. AM. CHEM. SOC., pp. 6164-6168 .

Srivastava R., and B. C. Yadav, 2012, Ferrite Materials: Introduction, Synthesis Techniques, and Applications as Sensors, International Journal of Green Nanotechnology, pp.141-154 .